

# CCQE-like $\nu_e$ selection in SBND with Convolutional Neural Network

Genevieve Breen<sup>1</sup>, Promita Roy<sup>2</sup>, Minerba Betancourt<sup>3</sup>, and Camillo Mariani<sup>2</sup>

<sup>1</sup>Department of Physics, Mount Holyoke College, South Hadley, MA 01075, USA

<sup>2</sup>Department of Physics, Virginia Tech University, Blacksburg, VA 24601, USA

<sup>3</sup>Fermi National Accelerator Laboratory, Batavia, IL 60510-5011, USA

August 5, 2025

## Abstract

The Short Baseline Neutrino program at Fermilab aims to study neutrino properties using three liquid argon time projection chamber detectors placed along the Booster Neutrino Beam (BNB). Neutrino charged-current quasi-elastic (CCQE) interactions occur when a neutrino collides with an argon nucleus, causing an ejected lepton and nucleon. CCQE interactions are the dominant mode at 1 GeV, which falls within the energy range of the BNB. Understanding of  $\nu_e$  CCQE interactions is crucial for accurate, in-depth neutrino-argon cross studies; however, this channel has not previously been studied in the Short Baseline Near Detector (SBND), the near detector in the program. Additionally, it is necessary to explore the efficacy of new event selection methods. We begin a CCQE-like  $\nu_e$  selection using simulated SBND neutrino events. We start with an inclusive  $\nu_e$  charged-current selection. This inclusive selection is the first in SBND to incorporate outputs from the Convolutional Visual Network (CVN), a neural network that classifies neutrino flavors from visual inputs. We then refine the inclusive  $\nu_e$  selection to events containing one electron, zero pions, and N protons, rejecting events based on Pandora particle identification  $\chi^2$  scores. We further restrict the selection to events containing one electron, zero pions, and one proton. We present one inclusive and two exclusive  $\nu_e$  signal selections with high signal purities, showing promise for the use of CVN in further SBND selection studies.

## 1 Introduction

### 1.1 The Short Baseline Neutrino Program

The Short Baseline Neutrino program is an experiment at the Fermi National Accelerator Laboratory (Fermilab) consisting of three detectors placed sequentially along the Booster Neutrino Beam (BNB) [1]. The experiment aims to reduce systematic uncertainties between the near and far detectors in order to conduct sterile neutrino searches, cross-section argon-neutrino studies, and new physics searches [1]. To date, electron neutrino selections have been conducted within the MicroBooNE and ArgoNeuT detectors [2] [3]. Only one exclusive selection of quasi-elastic-like (QE-like) electron neutrino interactions from the BNB has been conducted in the MicroBooNE detector [3]. The QE channel is the dominant interaction mode at 1 GeV, which falls within the BNB's energy range [2]. Understanding neutrino behaviour in this region is crucial in studying neutrino oscilla-

tion between the near and far detectors. The  $\nu_e$  CC inclusive selection used cuts based on the Convolutional Visual Network (CVN), a neural network that uses visual inputs neutrino flavour classification. This is the first use of CVN for SBND selection studies.

#### 1.1.1 Short Baseline Near Detector

The Short Baseline Near Detector (SBND) is the near detector in the SBN program, placed closest to the BNB target [1]. SBND collects data on the initial neutrinos in BNB for comparison with data collected at the far detector (ICARUS) [1]. All three detectors use Liquid Argon Time Projection Chamber (LArTPC) technology. A LArTPC is a volume filled with liquid argon, an inert material, between a cathode and an anode [1]. When a neutrino passes through the volume and interacts with an argon nucleus via the weak force, the outgoing charged particles ionize argon atoms, creating electron clouds that drift towards the cathode [1]. These electrons induce currents on three wire planes and are collected on a plate. Us-

ing information from the planes, the neutrino event can be reconstructed in three dimensions [1]. Additionally, photomultiplier tubes on the detector detect scintillation light emitted by the excited argon nuclei [1].

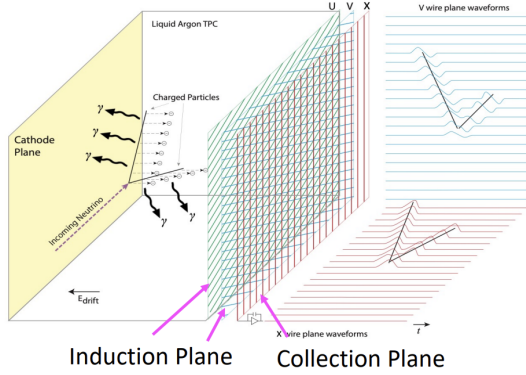


Figure 1: A diagram of a LArTPC detector depicting charged particles inducing currents on three wire planes [4].

## 1.2 Charged Current Quasielastic $\nu_e$ Selection

### 1.2.1 QE Interactions within SBND

Charged current quasi-elastic (CCQE) neutrino interactions occur when a neutrino collides with an argon nucleus, exchanging a  $W$  boson. A lepton and nucleon are ejected from the nucleus [5]. For  $\nu_e$  CCQE interactions, an electron and a nucleon exit the interaction vertex.

Within SBND, QE interactions can be detected by their final state charged particles. Different charged particles move differently through the argon; for example, a muon moves a longer distance than a proton. Some particles create a linear track, while other particles create showers of other particles. This can be seen visually in SBND’s event displays: track-like particles single lines while shower-like particles create multiple tracks with varying lengths and energies.

### 1.3 Convolutional Visual Network

The Convolutional Visual Network (CVN) is a convolutional neural network that takes in visual inputs (in this case, event displays) and outputs scores based on the event’s likelihood of being a  $\nu_e$  charged current (CC),  $\nu_\mu$  CC, neutral current (NC), and cosmic ray event [6]. An event is assigned four scores, each corresponding to a type of event and all adding up to 1 [6].

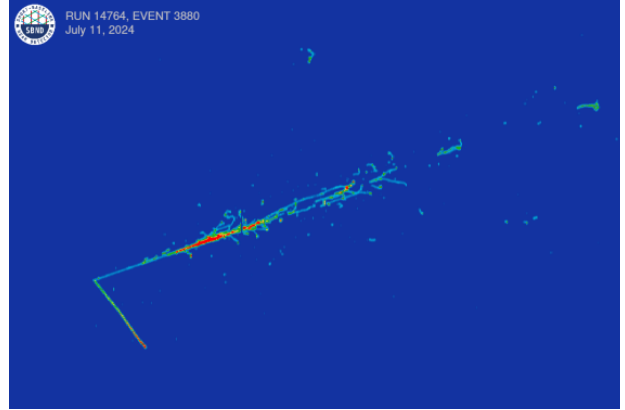


Figure 2: An event display from SBND depicting an electron neutrino quasi-elastic interactions. Two charged particles emerge from the neutrino interaction vertex: an electron shower above and a proton track below [6]

CVN is a newer method of event identification originally developed for the *NovA* experiment [6]. It has been previously used for the *ArgoNeuT* detector, and is currently being explored as a flavour classification tool for SBND and ICARUS [6].

### 1.4 Goal

This project aimed to begin a a CCQE-like selection for electron neutrinos within SBND, a previously unexplored channel in this detector. We pursued a final selection containing events with one electron and one proton. This entailed exploring and applying cuts to optimize both purity (the proportion of signal events in the final selection) and efficiency (the proportion of original signal retained).

## 2 Methods

### 2.1 Signal Definition

This selection study consisted of three stages, each selecting for a different signal. The first stage was a  $\nu_e$  charged current inclusive selection that excluded cosmic rays, neutral current, and muon neutrino interactions from the total signal. This selection also included preselection quality cuts. The second stage built upon the  $\nu_e$  CC inclusive cuts to select for a signal containing 1 electron, 0 pions, and  $N$  protons ( $1eNp0\pi$ ). The third stage restricted the number of protons to 1 ( $1e1p0\pi$ ). The final signal was defined as an interaction resulting in:

- 1 electron in the final state

- 1 proton in the final state
- 0 charged pions in the final state
- 0 neutral pions in the final state

## 2.2 Monte Carlo Sample

This selection used a Monte Carlo simulated sample created by the GENIE Event Generator, with overlaid cosmic rays generated by CORSIKA. Using a Monte Carlo simulation allows for us to determine the effectiveness of cuts with truth information before applying them to detector data. The simulation contains  $2.3 \times 10^{19}$  Protons on Target (POT) from the BNB. This sample consists of 95.8% cosmic rays, 3.2% muon neutrinos, 0.9% neutral current interactions, and 0.1% electron neutrinos. Some of the cuts used were provided by prior researchers or stored in the SBN Github, while others were created for this selection. The ROOT-based CAFAna framework was utilized for analysis.

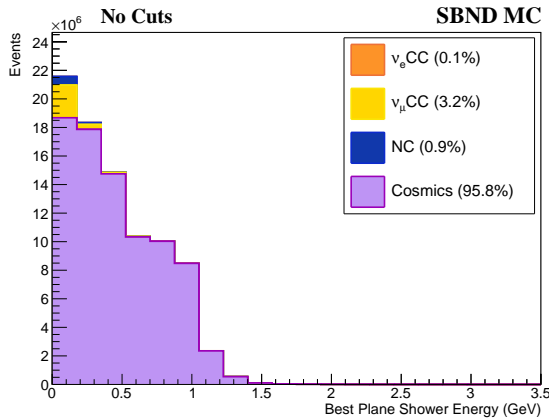


Figure 3: Best plane shower energy distribution for the Monte Carlo sample before any cuts. The electron neutrino signal is shown in orange.

## 2.3 $\nu_e$ CC Inclusive

### 2.3.1 Pre-selection Cut

First, we applied a pre-selection quality cut on the MC sample. As a prerequisite, events that occur within 20 centimetres of the detector walls were excluded, as outgoing particles that move outside of the argon volume may not be correctly identified. This fiducial volume containment cut only selected events in which the vertex and outgoing particles are all contained within the detector volume.

### 2.3.2 Cosmic Ray Rejection

Cosmic rays passing through the atmosphere and the earth also can enter the detector. After applying the pre-selection cut, we used cuts to reject cosmic rays. These dominated the initial sample, making up 95.8% of all events. In order to reject cosmic rays, we used two cuts. The first cut used the PandoraCosmic reconstruction chain to identify and reject events tagged as clear cosmic rays [7]. The second cut rejected events with an OptT0 score lower than 200. OptT0 flash-matching compares the measured scintillation light timing to the predicted timing based on TPC detection [8]. A higher score denotes a closer match; rejecting events with lower scores removes cosmic rays that do not match the predicted neutrino flash-matching [8].

### 2.3.3 $\nu_e$ Selection

In order to distinguish  $\nu_e$  events from  $\nu_\mu$  and neutral current events, we looked for events with an ejected electron.  $\nu_\mu$  events result in an ejected muon, while neutral current events result in no ejected lepton.

To select electron neutrinos, we selected events with the following topological cuts:

- Opening angle  $< 0.2$  radians
- Track length  $< 150$  cm
- Track score  $< 0.4$
- Conversion gap  $< 4$  cm
- Largest shower energy loss rate  $< 3$  MeV/cm

### 2.3.4 CVN Scores

We used CVN scores as our final set of inclusive selection cuts.

We applied cuts for all four scores:

- Selected any events with a  $\nu_e$  CC score over 0.9
- Rejected any events with a  $\nu_\mu$  CC score over 0.1
- Rejected any events with a nc score over 0.1
- Rejected any events with a cosmic score over 0.5

Applying these cuts resulted in a final  $\nu_e$  CC inclusive selection with a purity of 92.8% and an efficiency of 14.5%. All cosmic rays were removed from the selection, leaving a background of 3.4%  $\nu_\mu$  and 3.8% neutral current interactions.

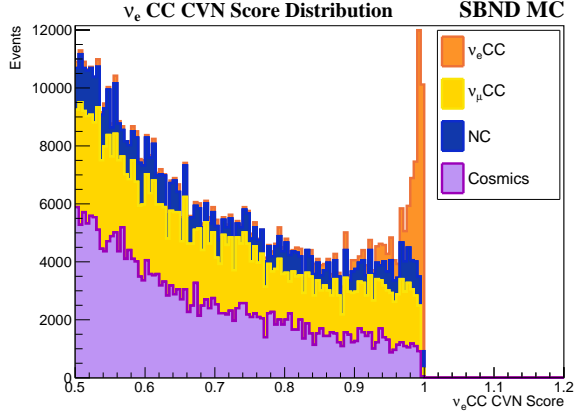


Figure 4:  $\nu_e$  CC CVN score distribution, with  $\nu_e$  shown in orange.

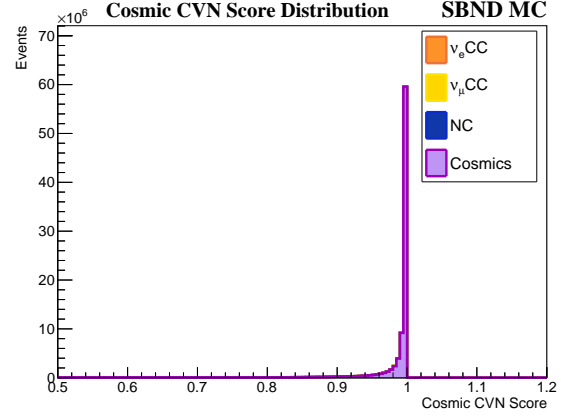


Figure 7: Cosmic CVN score distribution, with cosmics shown in purple.

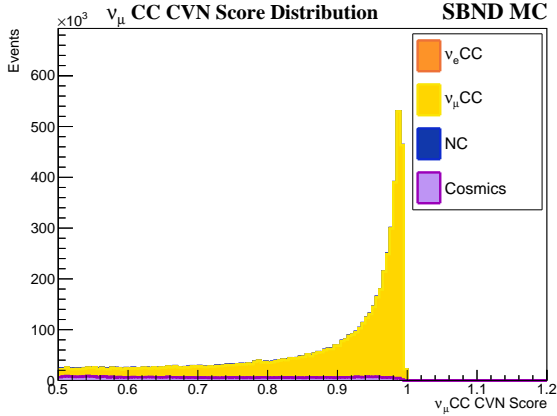


Figure 5:  $\nu_\mu$  CC CVN score distribution, with  $\nu_\mu$  shown in yellow.

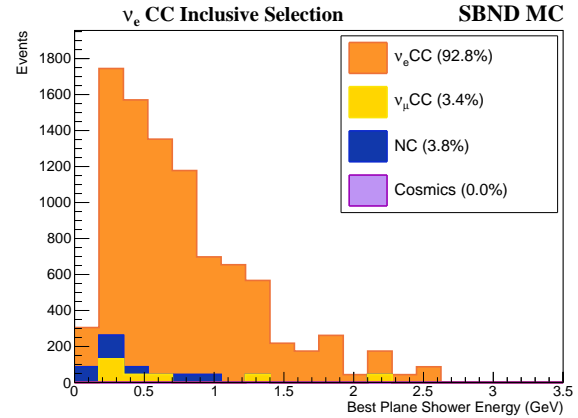


Figure 8: Best plane shower energy distribution for the  $\nu_e$  selection. The signal is shown in orange.

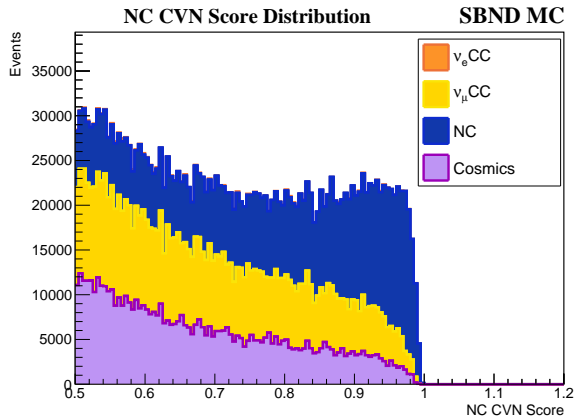


Figure 6: NC CVN score distribution, with NC shown in blue.

## 2.4 $1eNp1\pi$

The  $\nu_e$  CC inclusive selection can be separated into different interaction modes:

- Quasi-elastic (QE)
- Resonant (RES)
- Meson Exchange Current (MEC)
- Deep Inelastic Scattering (DIS)

Each interaction mode occurs at its own energy range, and results in different final state particles. The  $\nu_e$  CC inclusive selection already mostly contains QE interactions (54.9% purity). To increase the QE purity, we refined the initial  $\nu_e$  CC inclusive selection to select protons and reject pions in the final state. We explored multiple avenues for particle identification.

### 2.4.1 CVN Application

First, we examined CVN’s capabilities in identifying outgoing particles. The original CVN architecture developed for DUNE results in multiple outputs, each giving different information on an event’s characteristics. The third output of DUNE’s CVN contains scores for different numbers of protons, while the fourth and fifth output contain scores for different numbers of charged and neutral pions respectively [9].

However, SBND’s CVN is currently only trained for the first output, which we used for the  $\nu_e$  inclusive selection. In order to utilize CVN for further exclusive selections, the network would need to be trained on a new data set. Given the limited time of this project, it was not feasible to train CVN for use in particle identification. We turned to other methods already in use instead.

### 2.4.2 Pandora Particle ID

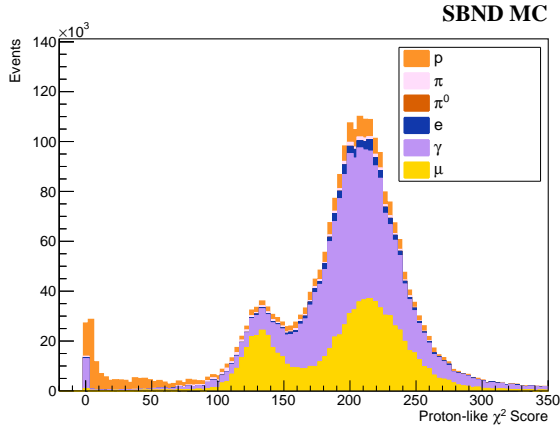


Figure 9: Proton-like  $\chi^2$  score distribution for individual particles. Protons are shown in orange.

We used Pandora particle identification for proton selection and pion rejection. Pandora is a software framework that uses a multi - algorithmic approach to event reconstruction and particle identification [7]. A reconstructed particle in Pandora has a vertex, parent and daughter particles, a track score, and associated 2D and 3D clusters and hits [7].

Pandora assigns a  $\chi^2$  score based on the likelihood of a track-like particle being a muon, a charged pion, or a proton. These scores are generated from topological information on particles emerging out of an identified interaction vertex by the PandoraNu reconstruction chain [7].

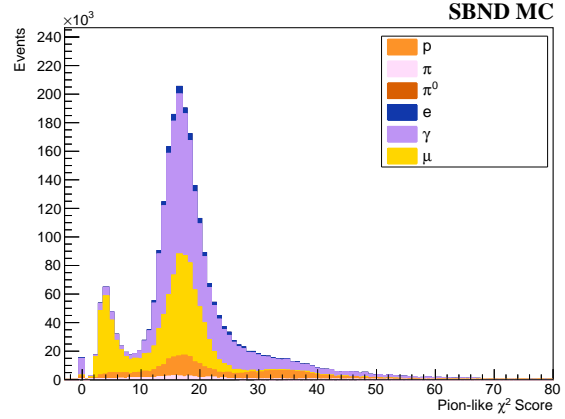


Figure 10: Pion-like  $\chi^2$  score distribution for individual particles. Protons are shown in orange, while pions are shown in pink.

### 2.4.3 $1eNp0\pi$ Selection Cuts

Initially, we plotted the proton-like, pion-like, and muon-like  $\chi^2$  scores for individual particles. We used these plots as guides for the cuts, then adjusted to improve purity and efficiency. For proton selection, we applied a cut including any event containing at least one track with a proton-like  $\chi^2$  score less than 90.

Rejecting pions proved less straightforward. For  $\chi^2$  pion-like scores, the pions and protons peak in the same region. The protons have an additional peak at higher  $\chi^2$  scores; however, cutting around this peak to exclude pions also results in a lower signal efficiency given the large amount of protons also excluded. We applied a cut excluding events containing tracks with a pion-like  $\chi^2$  score less than 16.

We explored cuts on muon-like  $\chi^2$  scores, but found that these decreased the selection’s efficiency without increasing purity, motivating us to focus solely on applying cuts based on pion and proton-like scores. Our cuts on proton and pion-like  $\chi^2$  scores also resulted in rejected muons, reducing the deep inelastic scattering (DIS) interactions in the MC sample.

Applying cuts for proton-like and pion-like  $\chi^2$  scores resulted in a  $1eNp0\pi$  selection with 88.7% purity and 16.5% efficiency.

## 2.5 $1e1p0\pi$

The  $1e1p0\pi$  selection entailed restricting the number of tracks identified as protons in the  $1eNp0\pi$  selection to 1. A cut was applied rejecting any events with more than one track with a proton-like  $\chi^2$  score below 90. As in the previous selection, any event containing

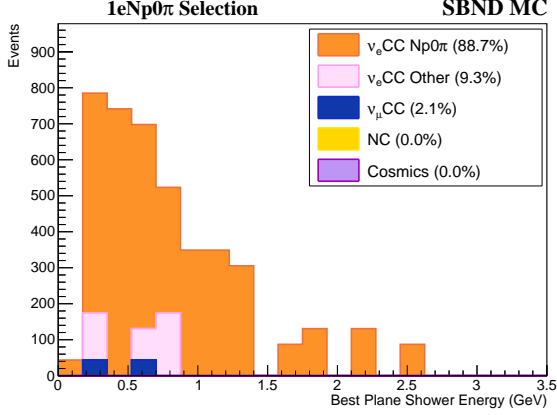


Figure 11: Best plane shower energy distribution for the 1eNp0 $\pi$  selection. The signal is shown in orange.

a track with a pion-like  $\chi^2$  score below 16 was also rejected. We opted to keep the  $\chi^2$  cuts at values as the previous selection because they returned high purity and efficiency.

### 3 Results and Analysis

#### 3.1 Final Selection

The final 1e1p0 $\pi$  selection yields a purity of 82.4% and an efficiency of 19.2%. The background contains no cosmic rays or neutral current events, with 2.7% of the total selection being charged current  $\nu_\mu$  and 14.9% being non-1p0 $\pi$   $\nu_e$  CC.

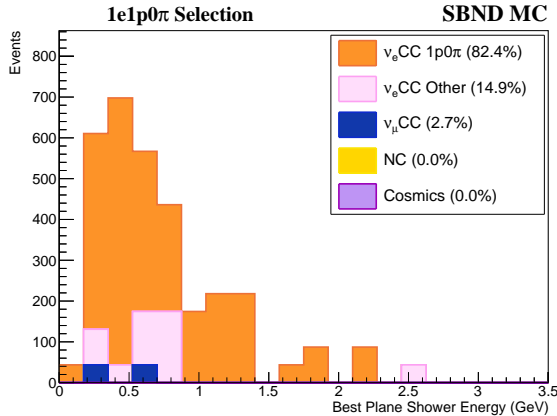


Figure 12: Best plane shower energy distribution for the 1e1p0 $\pi$  selection. The signal is shown in orange.

#### 3.2 Selection by Interaction Modes

This study intended to select CCQE-like interactions. When separating the  $\nu_e$  CC signal by interaction modes, the initial  $\nu_e$  CC inclusive selection yields a 54.9% QE signal purity. Selecting for N protons and 0 pions increases the QE purity to 64.2%, while selecting for 1 proton and 0 pions increases the purity to 75.0%.

In the final selection, the remaining background primarily consists of meson exchange current (MEC) interactions (15.3% purity). MEC interactions fall within the same energy region (around 1 GeV) as QE interactions, while resonant and deep inelastic scattering events peak at higher energies, resulting in a larger proportion of MEC interactions in the exclusive selections [5].

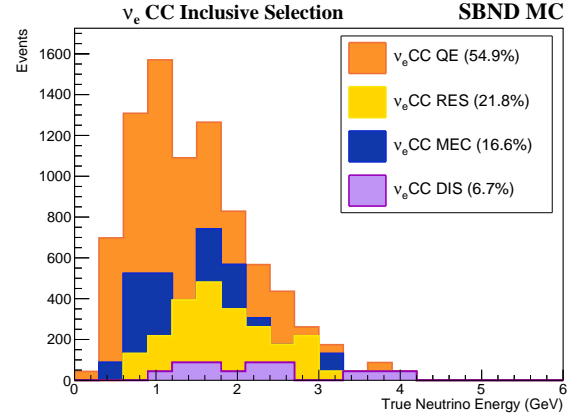


Figure 13: True neutrino energy distribution for  $\nu_e$  after applying  $\nu_e$  CC inclusive cuts, separated by interaction mode. The QE signal is shown in orange.

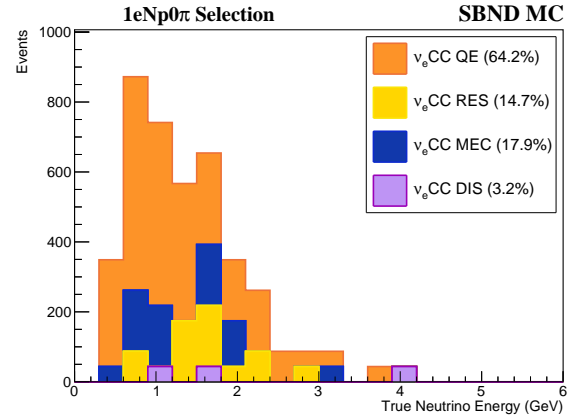


Figure 14: True neutrino energy distribution for  $\nu_e$  after applying 1eNp0 $\pi$  cuts, separated by interaction mode. The QE signal is shown in orange.

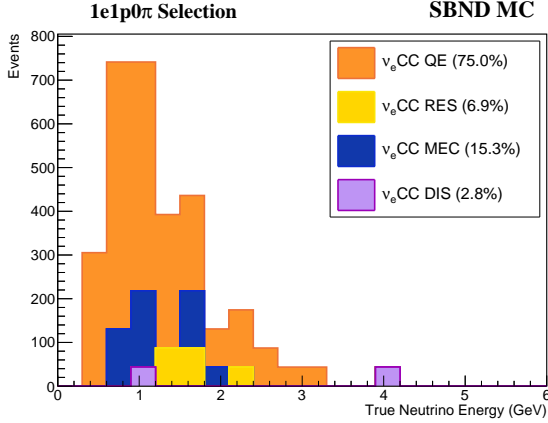


Figure 15: True neutrino energy distribution for  $\nu_e$  after applying  $1e1p0\pi$  cuts, separated by interaction mode. The QE signal is shown in orange.

## 4 Conclusion

The cuts used in this selection can be continually modified and added to in order to improve purity and efficiency in the selection. Next steps also include a comparison between this MC sample and detector data, and a measure of the selection uncertainties. A total GENIE uncertainty can also be determined using statistical fluctuation and GENIE reweight systematics:

$$\sigma_{total} = \sqrt{\sigma_{stat}^2 + \sigma_{genie\ reweight\ parameters}^2} \quad [10] \quad (1)$$

Additional sources of systematic uncertainty include neutrino flux and detector response. Further selection studies for this channel would include optimizing to reduce statistical uncertainty.

Pandora particle identification was used for the exclusive selections. However, given the high purity achieved in the  $\nu_e$  CC inclusive selection, CVN may also be a useful tool in selecting protons and rejecting pions. CVN particle identification has already been developed for DUNE, but would require training the neural network to produce outputs 3-5 (proton and pion identification) for SBND [9].

## 5 Acknowledgements

We acknowledge support from the National Science Foundation, the Virginia Tech Physics Department

and the Virginia Tech Center for Neutrino Physics. This work was made possible by the National Science Foundation under grant No. PHY-2149165.

Thank you to my REU advisor Camillo Mariani, SULI advisor Minerba Betancourt, and my mentors Promita Roy and Guadalupe Moreno for their immense support and invaluable guidance throughout this project. Special thanks to Hector Moya Freire for his work on the initial  $\nu_e$ CC analysis, Maria Artero Pons for help with CAFAna and selection cuts, and Supraja Balasubramanian for instruction in LArTPC technology and neutrino cross sections.

This document was prepared using the resources of the Fermi National Accelerator Laboratory (Fermilab), a U.S. Department of Energy, Office of Science, Office of High Energy Physics HEP User Facility. Fermilab is managed by FermiForward Discovery Group, LLC, acting under Contract No. 89243024CSC000002.

## References

- [1] P. A. Machado, O. Palamara, and D. W. Schmitz, “The short-baseline neutrino program at fermilab,” *Annual Review of Nuclear and Particle Science*, vol. 69, no. 1, pp. 363–387, Oct. 2019, ISSN: 1545-4134. DOI: 10.1146/annurev-nucl-101917-020949. [Online]. Available: <http://dx.doi.org/10.1146/annurev-nucl-101917-020949>.
- [2] M. A. Acero, M. Bustamante, P. B. Denton, S. J. Parke, and K. Wood, “First measurement of neutrino oscillation parameters using neutrinos and antineutrinos by nova,” *Phys. Rev. D*, vol. 106, p. L051102, 5 Sep. 2022. DOI: 10.1103/PhysRevD.106.L051102. [Online]. Available: <https://doi.org/10.1103/PhysRevD.106.L051102>.
- [3] A. Barnard, *Measurements of the differential charged-current cross section on argon for electron neutrinos with final-state protons in microboone*, Presented at: New Perspectives 2025, Fermilab, Jul. 2025. [Online]. Available: [https://indico.fnal.gov/event/68479/contributions/319812/attachments/189793/262083/abarnard\\_np\\_150725.pdf](https://indico.fnal.gov/event/68479/contributions/319812/attachments/189793/262083/abarnard_np_150725.pdf).
- [4] W. Wu, *Liquid argon time projection chambers for neutrino physics*, 2023. [Online]. Available: <https://lss.fnal.gov/archive/2023/slides/fermilab-slides-23-004-nd.pdf>.

- [5] A. V. Butkevich, “Reduced cross sections of electron and neutrino charged current quasielastic scattering on nuclei,” *Phys. Rev. C*, vol. 109, p. 045 502, 4 Apr. 2024. DOI: 10.1103/PhysRevC.109.045502. [Online]. Available: <https://link.aps.org/doi/10.1103/PhysRevC.109.045502>.
- [6] H. M. Freire, *Evaluation of the use of cvn scores for  $\nu_e$  cc selection*, SBND Cross-Section Meeting, SBN DocDB 40372, Apr. 2025. [Online]. Available: <https://sbn-docdb.fnal.gov/cgi-bin/sso/ShowDocument?docid=40372>.
- [7] I. Mawby, *Pandora pattern recognition overview*, Wire Cell Reconstruction Summit, Brookhaven National Laboratory, Apr. 2024. [Online]. Available: [https://indico.bnl.gov/event/21492/contributions/88557/attachments/53859/92119/PANDORA\\_BNL\\_12\\_04\\_24.pdf](https://indico.bnl.gov/event/21492/contributions/88557/attachments/53859/92119/PANDORA_BNL_12_04_24.pdf).
- [8] L. Tung, *First look at flash-matching using opt0finder in sbnd*, SBND Reco Meeting, SBN DocDB 38378, Oct. 2024. [Online]. Available: <https://sbn-docdb.fnal.gov/cgi-bin/sso/ShowDocument?docid=38378>.
- [9] DUNE Collaboration, “Neutrino interaction classification with a convolutional neural network in the dune far detector,” *Phys. Rev. D*, vol. 102, no. 9, p. 092 003, 2020, arXiv v2 (Nov 10, 2020). DOI: 10.1103/PhysRevD.102.092003. arXiv: 2006.15052 [physics.ins-det].
- [10] S. Yadav, *Inclusive  $\nu_\mu$  cc event selection with multi-topology splitting for oscillation analysis*, SBND Cross-Section Meeting, SBN DocDB 40873, Apr. 2025. [Online]. Available: <https://sbn-docdb.fnal.gov/cgi-bin/sso/ShowDocument?docid=40873>.